Mechanism of the Reaction of the $[W_3S_4H_3(dmpe)_3]^+$ Cluster with Acids: Evidence for the Acid-Promoted Substitution of Coordinated Hydrides and the Effect of the Attacking Species on the Kinetics of Protonation of the Metal-Hydride Bonds

Manuel G. Basallote,*[a] Marta Feliz,[b] M. Jesús Fernández-Trujillo,[a] Rosa Llusar,*[b] Vicent S. Safont,[b] and Santiago Uriel[c]

Abstract: The cluster $[W_3S_4H_3(dmpe)_3]^+$ (**1**) (dmpe = 1,2-bis-(dimethylphosphino)ethane) reacts with HX (X = Cl, Br) to form the corresponding $[W_3S_4X_3(dmpe)_3]^+$ (**2**) complexes, but no reaction is observed when **1** is treated with an excess of halide salts. Kinetic studies indicate that the hydride **1** reacts with HX in MeCN and MeCN–H_2O mixtures to form **2** in three kinetically distinguishable steps. In the initial step, the W–H bonds are attacked by the acid to form an unstable dihydrogen species that releases H_2 and yields a coordinatively unsaturated intermediate. This intermediate adds a solvent molecule (second step) and then replaces the coordinated solvent with X^- (third step). The kinetic results show that the first step is faster with HCl than with solvated H^+. This indicates that the rate of protonation of this metal hydride is determined not only by reorganization of the electron density at the M–H bonds but also by breakage of the H–X or H^+–solvent bonds. It also indicates that the latter process can be more important in determining the rate of protonation.

Keywords: cluster compounds · hydrides · kinetics · proton transfer · reaction mechanisms

Introduction

The chemistry of cuboidal metal clusters containing M_4Q_4 cores (M = metal; Q = O, S, Se) and their incomplete M_3Q_4 analogues has been a subject of interest over the last 20 years.[1] In addition to the Fe complexes, which are of particular relevance in bioinorganic chemistry, compounds containing Mo and W are useful molecular models in industrial hydrodesulfurization (HDS) catalysis.[2] Cubane-type transition metal sulfides and selenides are also a promising family of non-linear optical materials.[3,4] In the case of the incomplete M_3S_4 clusters, the Mo and W compounds are among the most studied, probably because of the easy preparation and stability of the $[M_3Q_4(H_2O)_9]^{4+}$ (M = Mo, W; Q = O, S, Se) aqua complexes.[1] Kinetic studies have revealed that a pH increase causes acceleration of the substitution reactions in these aqua complexes because of the formation of more labile conjugate–base hydroxocomplexes.[1,5,6] However, little is known about the properties of related hydride-containing clusters, except for the preparation of the $[W_3S_4H_3(diphosphine)_3]^+$ complexes (diphosphine = dmpe, depe, dppe) and their reactivity with benzoyl chloride that results in the formal substitution of H^- by X^-.[7] We have recently observed that $[W_3S_4H_3(dmpe)_3]^+$ (**1**) reacts with HX (X = Cl, Br) under mild conditions in a variety of solvents (acetonitrile, acetone and mixtures of these solvents with water) to also form the corresponding $[W_3S_4X_3(dmpe)_3]^+$ (**2**) halide complexes [Eq. (1)], whereas no reaction of **1** with an excess of halide salts is observed by NMR after several days.

$$[W_3S_4H_3(dmpe)_3]^+ + 3\,HX \rightarrow [W_3S_4X_3(dmpe)_3]^+ + 3\,H_2 \qquad (1)$$

These observations indicate that protons play an important role in the process and prompted us to carry out a kinetic study of these reactions. The study of the kinetics of

[a] Dr. M. G. Basallote, Dr. M. J. Fernández-Trujillo
Departamento de Ciencia de los Materiales e Ingeniería Metalúrgica y Química Inorgánica
Facultad de Ciencias, Universidad de Cádiz
Apartado 40, Puerto Real, 11510 Cádiz, (Spain)
Fax: (+34) 956-016-398
E-mail: manuel.basallote@uca.es

[b] M. Feliz, Dr. R. Llusar, Dr. V. S. Safont
Departament de Ciències Experimentals, Universitat Jaume I
Campus de Riu Sec, PO Box 224, 12080 Castelló (Spain)
Fax: (+34) 964-728-066
E-mail: llusar@exp.uji.es

[c] Dr. S. Uriel
Departamento de Química Orgánica- Química Física
Centro Politécnico Superior, Universidad de Zaragoza
María de Luna, 3, 50015 Zaragoza (Spain)

 DOI: 10.1002/chem.200305376

proton transfer to hydride complexes is a field of current interest and, to our knowledge, the results presented herein constitute the first report on the kinetics of proton transfer to a polynuclear metal hydride. In addition, the stability of **1** in water has also, for the first time, allowed kinetic information to be obtained about the relative rates of attack by the hydrated proton and undissociated HX molecules.

Results and Discussion

Kinetics of reaction of $[W_3S_4H_3(dmpe)_3]^+$ with acids: The kinetics of Equation (1) was initially studied in water–acetonitrile mixtures (volume ratio 3:1). Stopped-flow experiments using a diode-array detector revealed complicated spectral changes over time that indicate polyphasic kinetics of reaction. A satisfactory analysis of the data could be achieved by considering three consecutive kinetic steps with formation of two detectable reaction intermediates, ($\mathbf{I_1}$) and ($\mathbf{I_2}$), whose UV/Vis spectra are given in Figure 1. The final spectrum displays the band typical of the $[W_3S_4X_3(dmpe)_3]^+$ complexes, although the intensity of this band changes with the acid concentration, thus showing that the last kinetic step occurs under conditions of reversible equilibrium.

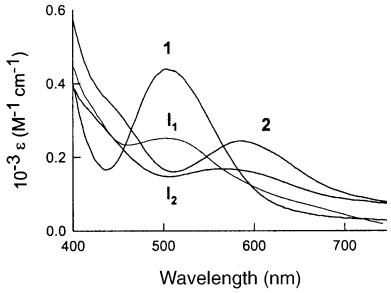

Figure 1. UV spectra of complex **1** and the intermediates formed in its reaction with HBr, as calculated from analysis of the spectral changes with time.

The rate constants corresponding to the initial step (k_{1obs}) change linearly with the acid concentration; the values are independent of the nature of the acid and remain unaffected by addition of an excess of X^- (Figure 2). The value derived for the second-order rate constant (k_1) from analysis of the whole set of data for different acids in H_2O/MeCN (3:1) is $(1.07 \pm 0.02) \times 10^2\ M^{-1}s^{-1}$ at 25 °C. In contrast, the rate constants for the second and third steps are independent of the nature and the concentration of both the acid and the X^- ion ($k_2 = 0.29 \pm 0.02\ s^{-1}$ and $k_3 = 0.019 \pm 0.004\ s^{-1}$ at 25 °C).

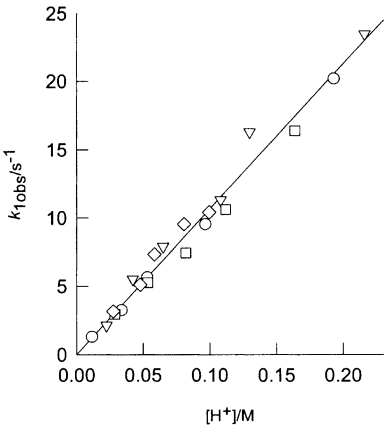

Figure 2. Plot of the observed rate constant for the first step in the reaction of $[W_3S_4H_3(dmpe)_3]^+$ with acids in acetonitrile–water (1:3 v/v) mixtures (25 °C, 0.50 M KNO_3). The plot includes data for the reaction with HCl (circles), HBr (triangles), HNO_3 (squares) and HCl in the presence of added KCl (diamonds). The solid line corresponds to the overall fit of the whole set of data.

The reaction of **1** with HNO_3 shows a first step with kinetics similar to that observed with HCl and HBr, but no spectral changes attributable to the k_2 and k_3 steps are observed. For this acid, following the initial step, there are slower and irreproducible absorbance changes that last for hours and lead to a reaction product with spectral characteristics that are very different from those of the remaining complexes studied in the present work (Data for the slow by-product: signals at $\delta = 55.3$ and 27.1 ppm in the ^{31}P NMR spectrum, no signals for coordinated hydrides in the ^1H NMR spectrum, shoulder at 450 nm in the UV/Vis spectrum). These spectral changes hinder the possible observation of steps corresponding to the k_2 and k_3 steps mentioned above. However, separate experiments showed that freshly prepared solutions of **1** and HNO_3 react with an excess of KCl to yield $[W_3S_4Cl_3(dmpe)_3]^+$ in a single kinetic step. The rate constant ($k_{obs} = 0.017 \pm 0.004\ s^{-1}$ (25 °C)) for this reaction is similar to that of k_3 in the reaction with HCl, indicating that intermediate $\mathbf{I_2}$ is also formed in the reaction with HNO_3. In contrast, no reaction with KCl is observed when the solutions of **1** and HNO_3 have been stored for hours, thus showing the slower formation of secondary products that are unreactive towards halide.

Abstract in Spanish: *El cluster $[W_3S_4H_3(dmpe)_3]^+$ (**1**) (dmpe = 1,2-bis(dimetillfosfino)etano) reacciona con los ácidos HX (X=Cl, Br) para formar los correspondientes complejos $[W_3S_4X_3(dmpe)_3]^+$ (**2**), pero no se observa reacción cuando se trata **1** con un exceso de sal. Los estudios cinéticos realizados indican que el hidruro **1** reacciona con HX en MeCN y mezclas MeCN–H_2O para formar **2** en tres etapas cinéticamente distinguibles: en la etapa inicial se produce el ataque del ácido a los enlaces W–H para formar un complejo de dihidrógeno inestable que libera H_2 y forma un intermedio coordinativamente insaturado que adiciona una molécula de disolvente (segunda etapa) y luego reemplaza el disolvente coordinado por el anión X^- (tercera etapa). Los resultados cinéticos muestran que la primera etapa es más rápida con la molécula de HCl que con el H^+ solvatado, lo que indica que la velocidad de protonación de este hidruro metálico está determinada no solo por la reorganización de la densidad electrónica sobre los enlaces M–H, sino también por la rotura de los enlaces H–X o H^+-disolvente, y que este último proceso puede llegar a ser el más importante a la hora de determinar la velocidad del proceso de protonación.*

Table 1. Kinetic data for the reaction of $[W_3S_4H_3(dmpe)_3]PF_6$ with acids in acetonitrile–water mixtures at 25.0 °C.[a]

% water in solvent	Ionic strength	Acid	k_1 [$M^{-1}s^{-1}$]	k_2 [s^{-1}]	k_3 [s^{-1}]
75	0.5 M (KNO_3)	HCl	$1.03(1)\times10^2$	0.28(1)	0.020(4)
		HCl(added Cl^-)[b]	$1.12(4)\times10^2$	0.28(2)	0.021(2)
		HBr	$1.13(4)\times10^2$	0.31(3)	0.017(4)
		HNO_3	$0.97(2)\times10^2$	[c]	[c]
		overall[d]	$1.07(2)\times10^2$	0.29(3)	0.019(4)
75	0.05 M (Bu_4NBF_4)	HCl	42(1)	[e]	0.009(1)
50		HCl	43(2)	[e]	0.016(2)
25		HCl	52(2)	[e]	0.026(3)
0[f]	0.05 M (Bu_4NBF_4)	HCl	$3.41(9)\times10^3$	0.18(3)	0.012(1)
		HCl (added Cl^-)[g]	$1.04(2)\times10^3$	[e]	0.010(2)
		DCl	$3.51(7)\times10^3$	0.17(3)	0.011(2)
		HBF_4	$2.53(6)\times10^2$	[e]	[h]

[a] The figures in parenthesis represent the standard deviation in the last significant digit. [b] Experiments in the presence of 0.27 M KCl with the ionic strength adjusted to 0.5 M with KNO_3. [c] Following the initial step, the reaction with HNO_3 leads to the slow formation of secondary products (see text). [d] Data corresponding to the overall fit of the data with all the acids in 0.5 M KNO_3; [e] No reliable values of the rate constant could be derived for this step. [f] Data in anhydrous acetonitrile. [g] Experiments in 0.05 M Bu_4NCl. [h] Following the initial steps there are very slow absorbance changes that lead to $[W_3S_4F_3(dmpe)_3]^+$ (see text).

Additional kinetic experiments were carried out in neat acetonitrile and in different acetonitrile–water mixtures. In some cases, three kinetic steps similar to those noted above could be resolved and the values of the rate constants are included in Table 1. However, reliable values of k_2 could not be obtained under certain conditions, mainly because the values of the observed rate constant for the first step become smaller and close to k_2. In acetonitrile–water mixtures, the values of k_1 only show small changes with the water content. Extrapolation of the data to neat water (0.05 M Bu_4NBF_4 ionic strength) leads to a value close to 40 $M^{-1}s^{-1}$ for the reaction of **1** with $H(H_2O)_n^+$ (The identity of protonated water in MeCN has been shown to be a mixture of $[H(H_2O)_n]^+$ species with $n=1$–4).[8]

In neat acetonitrile, k_1 is strongly dependent on the nature of the acid (Figure 3). For HBr, the process is too fast to give reliable kinetic data, whereas for HCl and HBF_4 quite different rate constants are obtained. The similar k_1 values for HCl and DCl indicate that the kinetic isotope effect is negligible. In the presence of added Cl^-, the values of k_1 for HCl show a clear deceleration (Figure 3), which indicates that the species reacting with **1** in this step is the HCl molecule. Actually, the data obtained with Cl^- in excess can be explained by considering the homoconjugation equilibrium [Eq. (2)], which has a K_h value (1.14×10^2) close to that reported in the literature (1.58×10^2).[9]

$$HCl + Cl^- \rightleftharpoons HCl_2^- \; ; \; K_h \qquad (2)$$

As the HBF_4 molecule is not stable and the formation of ion pairs is not favored in acetonitrile solution,[10,11] it appears reasonable to assume that the attacking species in this case is the acetonitrile-solvated proton (H^+_{MeCN}). In this case, the anion of the acid has a low coordinating ability; a species of the type $[W_3S_4(BF_4)_3(dmpe)_3]^+$ is thus not expected to be formed and the reaction thus stops with formation of the $\mathbf{I_2}$ intermediate. At the HBF_4 concentrations used in the kinetic experiments the values of k_{1obs} are in the range 0.2–1.5 s^{-1} and the values of k_2 are not well defined, so only k_1 is included in Table 1. Although NMR experiments showed the formation of $[W_3S_4F_3(dmpe)_3]^+$ (two doublets at $\delta=13.5$ and 10.3 ppm in the phosphorus spectrum with $J_{P,F}=57$ Hz and 92 Hz, respectively; one double doublet at $\delta=-203.0$ ppm in the fluorine spectrum with the same coupling constants) by abstraction of fluoride from the anion, this process occurs much more slowly than that of the stopped-flow measurements and does not cause any interference in the kinetic experiments.

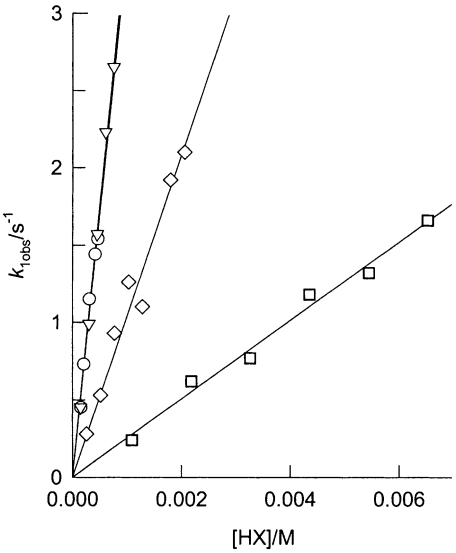

Figure 3. Plot of the observed rate constant for the first step in the reaction of $[W_3S_4H_3(dmpe)_3]^+$ with acids in neat acetonitrile (25 °C, 0.05 M Bu_4NBF_4). The plot includes data for the reaction with HCl (circles), DCl (triangles), HBF_4 (squares) and HCl in the presence of added Bu_4NCl (diamonds). The solid lines correspond to the fit of each set of data.

The nature of the reaction intermediates: With kinetic studies of reaction (1) completed, our efforts were directed toward determining the nature of the reaction intermediates. Although none of the intermediates could be isolated and structurally characterized, the nature of $\mathbf{I_2}$ could be clearly established as $[W_3S_4(H_2O)_3(dmpe)_3]^{4+}$ when there was water in the reaction medium. Thus, its spectrum in Figure 1 coincides with that obtained by treatment of a solution of the $[W_3S_4(OH)_3(dmpe)_3](PF_6)$ complex (**3**-PF_6), whose structure is described below, with HNO_3. The changes observed in the electronic spectrum of the latter complex after successive additions of KOH and HNO_3 are reversible and indicate the operation of the equilibrium represented in Equation (3). Moreover, kinetic experiments showed that **3** reacts with

HCl in MeCN-H_2O (1:3) solutions in a single kinetic step, with k_{obs} being independent of the acid concentration and having a value ($0.017 \pm 0.003\ s^{-1}$ at 25 °C) similar to that of k_3 under the same conditions.

$$[W_3S_4(OH)_3(dmpe)_3]^+ + 3\,H^+ \rightleftharpoons [W_3S_4(H_2O)_3(dmpe)_3]^{4+} \quad (3)$$

Additional evidence favoring the formulation of $\mathbf{I_2}$ as a triaqua complex in equilibrium with the corresponding trihydroxo complex was provided by NMR experiments. The phosphorus spectrum of a solution of **1** in [D_6]acetone containing an excess of HNO_3 displays two signals ($\delta = 9.8$ and -0.5 ppm) within the range observed for other $[W_3S_4X_3(dmpe)_3]^+$ complexes (X = H, Cl, Br). These signals can be assigned to intermediate $\mathbf{I_2}$ as, on addition of KBr, they disappear while signals of the $[W_3S_4Br_3(dmpe)_3]^+$ complex appear. On the other hand, complex **3** shows two signals at $\delta = 10.1$ and -5.3 ppm in [D_6]acetone solution, thus showing that $\mathbf{I_2}$ is not the trihydroxo complex. However, while the signal at $\delta = 10.1$ ppm is little affected by the addition of aliquots of an aqueous HNO_3 solution, the chemical shift for the other signal changes significantly up to about +2 ppm. As shown in Figure 4, these changes can be reversed by the addition of KOH, which indicates again the

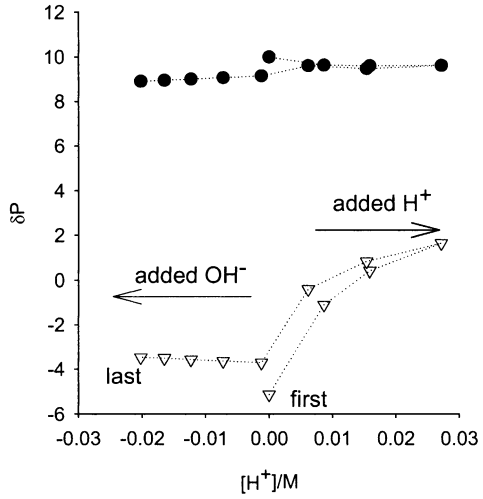

Figure 4. Plot of the changes with the concentration of added HNO_3 and KOH to a solution of complex **3**-PF_6 in [D_6]acetone at 25 °C. As the acid and base were added in aqueous solution, the differences between the chemical shifts observed in the first and last spectra are most likely caused by a change in the composition of the solvent.

operation of the equilibrium in Equation (3). Thus, the $\mathbf{I_2}$ intermediate observed during the course of the reaction of **1** with acids can be considered to be $[W_3S_4(H_2O)_3(dmpe)_3]^{4+}$ in equilibrium with the corresponding trihydroxo complex, the relative amounts of both species depending on the actual concentration of acid. As the spectrum of intermediate $\mathbf{I_2}$ in neat MeCN is very similar to that observed in the presence of water, it appears reasonable to consider that the intermediate formed under these conditions is $[W_3S_4(MeCN)_3(dmpe)_3]^{4+}$ and that the last step in the mechanism of reaction (1) consists of the substitution of coordinated solvent by the X^- ion.

However, the most interesting fact in the mechanism of reaction (1) resides in the nature of intermediate $\mathbf{I_1}$, for which the electronic spectrum is independent of the nature of both the acid and the solvent. As kinetic data indicate that $\mathbf{I_1}$ is formed by reaction of **1** with acid, reasonable possibilities for H^+ (or HX) attack include direct attack at the W–H bonds and labilisation of the coordinated hydrides by protonation of the μ_2- or μ_3-S^{2-} bridges. Theoretical calculations were carried out to discriminate between these possibilities. The results showed that protonation at the W–H bond is favored by 11.89 kcal mol^{-1} with respect to protonation at μ_2-S^{2-} and by 31.42 kcal mol^{-1} with respect to protonation at μ_3-S^{2-}. The optimized geometry of the resulting product (Figure 5) clearly differs from that of a classical dihydride and it is best described as a dihydrogen complex

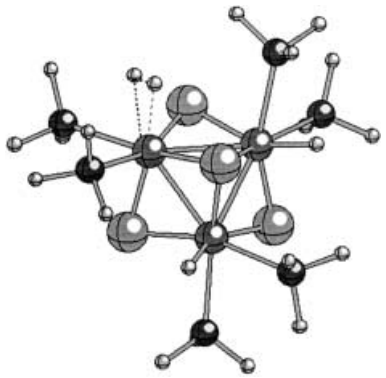

Figure 5. Optimized geometry for the intermediate resulting from H^+ attack to one of the W–H bonds in the $[W_3S_4H_3(PH_3)_6]^+$ model complex.

with a short H–H distance (0.78 Å). Although there is no previous report of W^{IV} dihydrogen complexes, their formation as transient species has previously been proposed.[12]

To confirm the nature of this intermediate, the early stages of reaction (1) were monitored by using low temperature NMR spectroscopy. For this purpose, the reaction with HBF_4 was initially selected because at short reaction times it stops with the formation of the $\mathbf{I_2}$ intermediate. When the reaction with this acid is carried out in CD_3CN at 0 °C, the NMR spectra show the sequential formation of three products containing two, one, and zero W–H bonds, but no signal for coordinated H_2 is observed. For the intermediate with two W–H bonds: $\delta_H = -0.19$ ppm ($^2J_{H,P} = 49$ and 31 Hz) and -0.22 ppm ($^2J_{H\text{-}P} = 46$ and 30 Hz), $\delta_P = 12.8$, 10.6, 7.3, 1.6, -1.7 and -11.4 ppm; for the intermediate with a single W–H bond: $\delta_H = -0.02$ ppm ($^2J_{H,P} = 49$ and 30 Hz), $\delta_P = 11.8$, 10.6, 9.4, 6.6, -0.5 and -3.3 ppm; for the third intermediate there are no hydride signals and $\delta_P = 7.5$ and -2.2 ppm. The actual values of the chemical shifts are temperature-dependent; when the temperature is changed, changes of up to 0.15 ppm in the ^1H spectra and 1.5 ppm in the ^{31}P spectra are observed for both the starting complex and the intermediates. Importantly, the phosphorus spectra for the intermediates containing two or one W–H bonds show six signals as a consequence of the symmetry decrease caused by reac-

tion at only one or two metal centers. When the reaction at the three metal centers is completed, the symmetry is recovered and only two signals are observed in the phosphorus spectra.

These results can be interpreted by considering that each kinetic step in the stopped-flow experiments corresponds to a different chemical process that occurs sequentially at the three metal centers, with statistically controlled kinetics. It can easily be demonstrated[13] that, if the metal centers behave as independent chromophores and the rate constants are statistically controlled (3:2:1 ratio in the present case), the kinetic traces can be fitted by a single exponential with an apparent rate constant that corresponds to that of the slowest step, that is, to the reaction at the third metal center. Statistically controlled kinetics has previously been reported for several reactions of polynuclear metal complexes,[14] including some reports by the group of Sykes on substitution reactions in incomplete M_3Q_4 clusters.[1,5,6,15] According to this interpretation, under the experimental conditions of the NMR experiments, only the three forms corresponding to intermediate $\mathbf{I_2}$ are formed in the reaction with HBF_4. This conclusion was confirmed by NMR experiments using a deficit of HBF_4, which showed the exclusive formation of the $\mathbf{I_2}$ intermediate with two W–H bonds. When HBF_4 is replaced by HCl, the spectra (CD_3CN, 0 °C, deficit of acid) of the first intermediate [$\delta_H = -0.10$ ppm ($^2J_{H,P} = 48$ and 32 Hz) and -0.42 ppm ($^2J_{H,P} = 44$ and 28 Hz), $\delta_P = 12.8$, 9.8, 4.7, -0.1, -3.6 and -10.1 ppm] are slightly different and favor its formulation as $[W_3S_4H_2Cl(dmpe)_3]^+$. These results indicate that, at 0 °C and using a deficit of acid, the relative rates of the different kinetic steps change with respect to those observed in the stopped-flow experiments at 25 °C, and the first step becomes rate-determining. For this reason, only the product corresponding to the occurrence of the three consecutive steps at a single metal center is observed.

In new attempts to detect the dihydrogen intermediate suggested by the theoretical calculations, the reaction with a deficit of HBF_4 was examined at -70 °C in [D_6]acetone. In this case, two distinct intermediates containing two W–H bonds were detected ($\delta_H = -0.21$ ppm with $^2J_{H,P} = 40$ and 32 Hz, and -0.70 ppm with $^2J_{H,P} = 52$ and 28 Hz for one of the intermediates, and $\delta_H = -0.23$ ppm with $^2J_{H,P} = 44$ and 32 Hz, and -0.59 ppm with $^2J_{H,P} = 44$ and 28 Hz for the other one), but again no signal assignable to a dihydrogen complex could be observed. If one of the intermediates ($\mathbf{I_2}$) is considered to contain coordinated solvent at the coordination site originally occupied by H^- in one of the metal centers, the problem is to determine the nature of the ligand occupying that coordination site in the other intermediate. Multiple NMR experiments using different acids, solvents, and temperatures were unsuccessful in detecting any dihydrogen signal, so we decided to look for an alternative explanation. We carried out theoretical calculations to determine the energy difference between the dihydrogen structure in Figure 5 and the product resulting from H_2 dissociation. The results indicate that the process [Eq. (4)] only requires 1.8 kcal mol^{-1}, so it would be driven under the experimental conditions by the favorable entropy change. According to this result, intermediate $\mathbf{I_1}$ would be a coordinatively unsaturated complex containing a vacant coordination site at the position originally occupied by the hydride. (There would, actually, be three $\mathbf{I_1}$ intermediates formed with statistically controlled kinetics and corresponding to reaction at one, two or three metal centers).

$$[W_3S_4H_2(H_2)(dmpe)_3]^{2+} \rightarrow [W_3S_4H_2(dmpe)_3]^{2+} + H_2 \qquad (4)$$

The crystal structure of the $[W_3S_4(OH)_3(dmpe)_3](BPh_4)\cdot CH_2Cl_2$ complex: The structure of $[W_3S_4(OH)_3(dmpe)_3](BPh_4)\cdot CH_2Cl_2$ was determined by single-crystal X-ray diffraction experiments. The main features of the structure are similar to those reported for other M_3Q_4 compounds with incomplete cuboidal type geometries. A drawing of the cation **3** together with the atom-numbering scheme is shown in Figure 6. With space group $P\bar{1}$ and one entire molecule per asymmetric unit, there is not crystallographic symmetry imposed on the cation; however, the molecule has an effective C_3 symmetry. Table 2 contains a list of the most important averaged bond lengths together with those reported for the cations $[W_3S_4Cl_3(dmpe)_3]^+$ and $[W_3S_4H_3(dmpe)_3]^+$ for comparative purposes.[7] The chloride derivative has been chosen instead of the $[W_3S_4Br_3(dmpe)_3]^+$ precursor because substitution of Br by Cl does not affect the metal–metal, metal–sulfur and metal–phosphorus distances and the quality of the structural parameters reported for the chloride cluster is much higher.

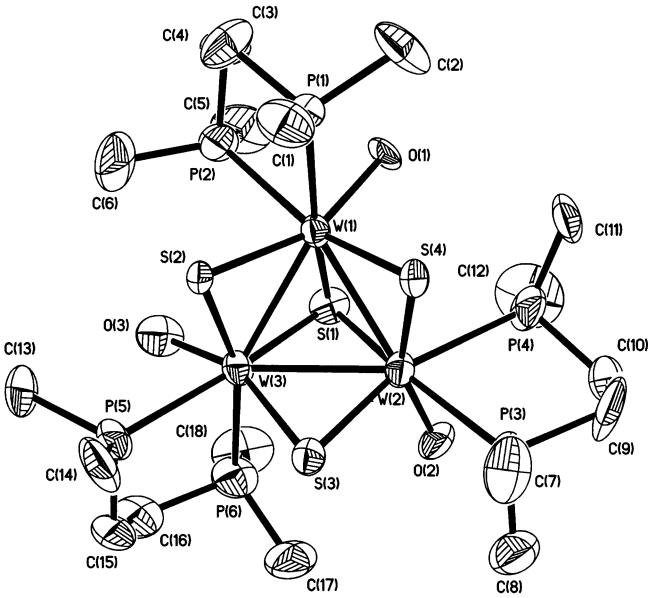

Figure 6. ORTEP representation of $[W_3S_4(OH)_3(dmpe)_3]^+$ (50% probability ellipsoids) with atom numbering scheme.

The metal–metal distances in Table 2 are consistent with a metal oxidation state of IV and with the substitution of the halide ion coordinated to the metal by a hydroxy group. The metal–oxygen bond length of 2.100(6) agrees with this formulation. Similar distances have been observed for the

Table 2. Selected averaged bond lengths [Å] for trinuclear clusters with $[W_3S_4]$ units.[a]

Length [Å]	$[W_3S_4Cl_3(dmpe)_3]^+$[7]	$[W_3S_4H_3(dmpe)_3]^+$[7]	$[W_3S_4(OH)_3(dmpe)_3]^+$
M–M	2.755(1)	2.751[4]	2.769[10]
M–μ_3-S(2)	2.382(5)	2.354[2]	2.385[11]
M–μ-S(2)[b]	2.288(5)	2.341[4]	2.331[4]
M–μ-S(2)[c]	2.327(3)	2.329[8]	2.343[10]
M–μ-S(2)$_{av}$	2.308[14]	2.335[9]	2.337[8]
M–OH (or Cl)	2.488(4)	–	2.100[6]
M–P(1)	2.520(4)	2.476[9]	2.513[18]
M–P(2)	2.595(3)	2.516[5]	2.589[12]

[a] Standard deviations for averaged values are given in square brackets. [b] Mo–μ-Q distance *trans* to Mo–X bond. [c] Mo–μ-Q distance *trans* to Mo–P(2) bond.

oxygen atoms in the alkoxo groups attached to molybdenum in the $[Mo_3S_4(tdci)_3]^{4+}$ complex (tdci = 1,3,5-tris(dimethylamino)-*cis*-inositol), with an average Mo–O value of 2.087 Å, compared with M–H_2O distances in $[M_3S_4(PPh_3)_3Cl_4(H_2O)_2]$ of about 2.25 Å for M = W and 2.27 Å for M = Mo.[16–18]

The replacement of a halide by an hydroxy group is also reflected in the metal–bridging chalcogenide distances. The differences in the M–μ_2-Q distances, attributed to the larger trans-effect of the phosphine versus the halide or hydroxide, in $[W_3S_4Cl_3(dmpe)_3]^+$ and $[W_3Se_4Br_3(dmpe)_3]^+$, are 0.04 Å compared with the 0.012 Å observed for **3**. Substitution of a hydroxy group by hydrogen lengthens the W–μ_2-S distance roughly *trans* to that position by about 0.01 Å and shortens by the W–μ_2-S distance *trans* to the phosphorus atom by about 0.01 Å.

The mechanism of reaction of the $[W_3S_4H_3(dmpe)_3]^+$ cluster with acids: The whole set of experimental findings in the present paper can be rationalized according to the mechanism in Equations (5)–(8), where, for simplicity, only reaction at one of the metal centers is considered. A complete description of the mechanism is more complicated but can be easily obtained from these equations by simply considering that each step actually includes three steps, corresponding to the sequential reaction at the three metal centers. Moreover, because of the statistically controlled kinetics, the rate constants for the different steps can also be easily derived from the experimental values by considering that they are in a 3:2:1 ratio. As the values derived from the experimental kinetic traces correspond to the slowest one,[13] the rate constants for reaction at the first metal center are 3 k_1, 3 k_2, and 3 k_3, as indicated in Equations (5)–(8).

$$[W_3S_4H_3(dmpe)_3]^+ + HX \rightarrow [W_3S_4H_2(H_2)(dmpe)_3]^{2+} + X^-;\ 3k_1 \quad (5)$$

$$[W_3S_4H_2(H_2)(dmpe)_3]^{2+} \rightarrow [W_3S_4H_2(dmpe)_3]^{2+} + H_2;\ \text{fast} \quad (6)$$

$$[W_3S_4H_2(dmpe)_3]^{2+} + \text{solv} \rightarrow [W_3S_4H_2(solv)(dmpe)_3]^{2+};\ 3k_2 \quad (7)$$

$$[W_3S_4H_2(solv)(dmpe)_3]^{2+} + X^- \rightarrow [W_3S_4H_2X(dmpe)_3]^+;\ 3k_3 \quad (8)$$

The initial attack [Eq. (5)] occurs with formation of an unstable dihydrogen complex that rapidly dissociates H_2 [Eq. (6)] to form a coordinatively unsaturated intermediate $\mathbf{I_1}$. The process represented in Equation (5) could actually be more complicated as it can occur through the formation of W–H···H–X dihydrogen-bonded intermediates. In fact, several examples of this type of adduct have been reported in recent years as intermediates in proton-transfer processes.[19] Once the $\mathbf{I_1}$ intermediate has been formed, the reaction continues with solvent addition to the vacant coordination site [Eq. (7)] to form intermediate $\mathbf{I_2}$, which substitutes the anion of the acid for the coordinated solvent in the last step [Eq. (8)]. As the last step is a simple substitution reaction, according to the Eigen–Wilkins mechanism a saturation behavior is expected for the k_{3obs} values. In the present case, the rate constants for substitutions of coordinated solvent in intermediate $\mathbf{I_2}$ by Cl^- and Br^- are independent of $[X^-]$, and only lead to the value of the limiting rate constant. In contrast, substitutions in related $[M_3Q_4(H_2O)_9]^{4+}$ complexes usually exhibit a first-order dependence on $[X^-]$,[1,5,6] although the concentrations of the entering ligand usually employed in those studies are much smaller than those in the present work. Unfortunately, in the present system, kinetic data for this substitution process could not be obtained at lower concentrations of X^-, as the third step in the reaction of **1** with acids occurs under conditions of reversible equilibrium and the formation of the $[W_3S_4X_3(dmpe)_3]^+$ species requires high concentrations of the anion.

A somewhat confusing conclusion of the proposed mechanism is that addition of a solvent molecule to the vacant coordination site [Eq. (7)] is a relatively slow process (k_2 = 0.17–0.31 s^{-1}). Nevertheless, there are previous reports of additions to coordinatively unsaturated complexes occurring at similar rates.[20,21] In those cases, the low reaction rates have been interpreted by considering a stabilization of the unsaturated complex, either by formation of agostic bonds[20] or by an increased σ-donation from the ancillary phosphine ligands.[21] To check the latter possibility, we carried out a comparative study of the bond lengths in the optimized geometries of the model complex $[W_3S_4H_3(PH_3)_6]^+$ and the analogous compound $[W_3S_4H_2(PH_3)_6]^{+2}$, which has a vacant coordination site at one of the W atoms. The results showed that the major change corresponds to the distance between the unsaturated metal center and the μ_2-S^{2-} *trans* to the hydride, which is 0.093Å shorter in the complex with the vacant site. Other changes in the bond lengths are considerably smaller and can hardly be invoked to explain a stabilization of the unsaturated complex. The whole set of theoretical calculations therefore suggest that intermediate $\mathbf{I_1}$ most probably contains a vacant coordination site (resulting from H_2 dissociation) and that this structure is stabilized by an increase in electron donation from the sulfide *trans* to the vacant site. This stabilization would lead to a higher energy barrier for solvent addition and, hence, conversion to $\mathbf{I_2}$ would be a relatively slow process detectable in the kinetic experiments.

According to the mechanism in Equations (5)–(8), the acid-promoted substitution of H^- in the incomplete cube **1** [Eq. (1)] is a consequence of consecutive protonation and

H_2-elimination processes. The present results provide, for the first time, kinetic support to the possibility of acid-accelerated substitutions in W-S cubes. This behavior would be very different from that previously observed for substitutions in the related aqua complexes, for which substitutions become faster with decreasing acidity, due to the formation of more labile hydroxo complexes.[1,5,6] Although a first-order term in $[H^+]$ has been observed for the formation of $[Mo_3Q_4(H_2O)_9]^{4+}$ by abstraction of Q from $[Mo_3Q_7(H_2O)_6]^{4+}$, no acceleration with increasing $[H^+]$ is observed for substitution of coordinated water in the latter complexes.[6] In contrast, the existence of acid-catalyzed substitutions in analogous Fe clusters is well illustrated.[22] There is, however, a major difference between the clusters of both metal ions with respect to the mechanism of the acid-promoted acceleration: whereas in the Fe complexes it is caused by labilization of the departing ligand (induced by protonation of the bridging sulfides), the acceleration observed in **1** is caused by protonation at metal–hydride bonds.

It is also important to note that the rate of acid attack at the M–H bonds strongly depends on the nature of the attacking species. This is also of relevance for the protonation of other metal hydrides, including those leading to the formation of stable dihydrogen complexes. Although this dependence has previously been demonstrated for the reaction of other hydride complexes with HX molecules in tetrahydrofuran solution,[10,23–25] the present results extend this conclusion to other solvents and allows, for the first time, comparison of the relative rates of protonation with HX molecules and the solvated proton. According to the data in Table 1, the rate of protonation follows the order HX > H^+_{MeCN} > $H^+_{H_2O}$, that is, attack by the HCl molecule is faster than attack by the solvated proton, with the slowest reaction being observed for the hydrated proton. This result contrasts with the ideas derived from the behavior of classical acids and bases in aqueous solution, for which the rate of proton transfer increases with the difference in acidity between the reagents,[23,26] the fastest protonation of a base corresponding to reaction with the strongest acid, that is, the solvated proton. The reversed ordering observed for protonation of **1** is thus unexpected and confirms previous suggestions that the acid–base behavior of the metal hydrides can not be easily extrapolated from that of classical acids and bases in aqueous solution.[27] The reason for this singular behavior resides in the fact that protonation of a coordinated hydride occurs through transition states with M–H···H–X (or M–H···H^+_{solv}) links and reorganization of the electron density at both the M–H and the H–X(or H^+–solvent) bonds contribute to the rate of reaction. The present results indicate that, at least in some cases, the breaking of the H^+–solvent bonds can represent the most important contribution to the activation barrier of the protonation process.

Experimental Section

Materials: The molecular triangular clusters $[W_3S_4H_3(dmpe)_3](PF_6)$ and $[W_3S_4Br_3(dmpe)_3](PF_6)$ were prepared according to literature methods.[7,28] Other reactants were obtained from commercial sources and used as received. Solvents for synthesis were dried and degassed by standard methods before use.

Physical measurements: Elemental analyses were carried out with a C. E. analyzer, model EA 1108. IR spectra were recorded on a Perkin Elmer System 2000 FT-IR using KBr pellets. Electrospray mass spectra were recorded on a Micromass Quattro LC instrument using nitrogen as the drying and nebulising gas. NMR experiments were performed on Jeol EX400, Bruker Avance 600 and Varian Unity 400 spectrometers. For monitoring of the protonation reaction at low temperatures, the samples were placed in tubes provided with screw-cap septa and cooled inside the magnet at the desired temperature, prior to addition of the acid solutions. For the experiments in CD_3CN and acetone-d_6, the solutions of HCl and HBr were generated from MeOH and $ClSiMe_3$ or $BrSiMe_3$.

Kinetic experiments: The experiments were carried out at 25.0 °C using an Applied Photophysics SX17-MV stopped-flow spectrophotometer provided with a diode-array detector. In all cases, solutions of the starting complex in the desired solvent were mixed, in the instrument, with solutions of the acid in the same solvent. Both solutions contained the amount of salt required to maintain a constant ionic strength. The concentration of acid was determined in each case by titration with a previously standardized KOH solution; for the acid solutions in MeCN, titration was carried out after diluting an aliquot (1–5 mL) with water (50 mL). For the kinetic experiments in neat MeCN, and for the NMR experiments in the same solvent and $[D_6]$acetone, HCl was generated by reaction of $ClSiMe_3$ with MeOH and DCl was generated by reaction of $ClSiMe_3$ with MeOD. HBr was generated in a similar fashion from $BrSiMe_3$. Most kinetic experiments were carried out using the diode-array detector and the results were analyzed with the GLINT program.[29] In some cases, the experiments were carried out at a single wavelength and the kinetic traces were analyzed with the standard software of the stopped-flow instrument.

Theoretical calculations: Calculations were performed on a model $W_3S_4H_3(PH_3)_6^+$ complex with the Becke hybrid density functional (B3LYP)[30,31] method using the Gaussian 98 program.[32] B3LYP has been used in conjunction with the double-ζ pseudo-orbital basis set LanL2DZ, in which the metal atoms are represented by the relativistic effective core LanL2 potential of Los Alamos.[33]

Synthesis of $[W_3S_4(OH)_3(dmpe)_3](PF_6)$ (3-PF_6): A blue solution of $[W_3S_4Br_3(dmpe)_3](PF_6)$ (200 mg, 0.132 mmol) in CH_3CN/H_2O (1:1, 120 mL) was treated dropwise with 0.1 M NaOH (10 mL, 1 mmol) and the mixture was stirred at room temperature for 4 h. After removing some of the solvent (ca. 60 mL) under reduced pressure, the desired product was extracted with CH_2Cl_2 (60 mL × 3) and the resulting pink organic solution was dried with $MgSO_4$, filtered, and concentrated under reduced pressure. Addition of diethyl ether to the above solution precipitated the desired product, which was then separated from the solution by filtration. The solid was dried to give $[W_3S_4(OH)_3(dmpe)_3](PF_6)$ as an air-stable pink product (yield 105 mg; 60 %). Elemental analysis calcd for $W_3S_4P_7C_{18}H_{51}O_3F_6$: S 9.67, C 16.30, H 3.88; found: S 9.81, C 16.72, H 3.79; $^{31}P\{^1H\}$ NMR (CD_3CN): $\delta = -144.2$ (septet, 1P, $^1J(^{31}P,^{19}F) = 704.0$ Hz), −5.62 (s, 3P, $^1J(^{31}P^{183}W) = 169.2$ Hz), 9.47 (s, 3P, $^1J(^{31}P,^{183}W) = 204.0$ Hz); IR (KBr): $\tilde{\nu}$1417 (s, P-CH_2), 1300(m), 1287 (m, P-CH_3), 1136 (m, CH_3), 993 (w), 950 (s, CH_3), 939 (s), 898 (s, CH_3), 840 (s, P-F), 808 (m), 752 (m, CH_2), 714 (m, CH_2), 652 (m), 557 (s, P-F), 495 (s, W-O), 433 (m, W-μ_3-S), 338 cm^{-1} (m); UV/Vis (CH_3CN): $\lambda = 517$ (b), 317 (b), 260 nm (sh); electrospray-MS (CH_3CN, 75 V, m/z): 1181 ($[M^+]$), 1163 ($[M^+ - H_2O]$), 1031 ($[M^+ - dmpe]$), 1013 ($[M^+ - dmpe - H_2O]$).

X-ray data collection and structure refinement: Suitable crystals for X-ray studies of the tetraphenylborate salts of **3** were grown by slow diffusion of diethyl ether into a sample solution in CH_2Cl_2. Replacement of the PF_6^- ion was carried out by addition of an excess of $Na(BPh_4)$ to methanol solutions of **3**-PF_6, resulting in precipitation of the desired tetraphenylborate salts of the trinuclear cation **3**. The crystals are air-stable and were mounted on the tip of a glass fibre with the use of epoxy cement. X-ray diffraction experiments were carried out on a Bruker SMART CCD diffractometer using $Mo_{K\alpha}$ radiation ($\lambda = 0.71073$ Å). The data were collected with a frame width of 0.3° in Ω and a counting time of 25 s per frame at a crystal–detector distance of 4 cm. SAINT software was used for integration of intensity reflections and scaling and SADABS

Table 3. Crystallographic data for $[W_3S_4(OH)_3(dmpe)_3](BPh_4)\cdot CH_2Cl_2$

Compound	**3**-$BPh_4\cdot CH_2Cl_2$
empirical formula	$C_{43}H_{73}BC_{l2}O_3P_6S_4W_3$
formula weight	1585.33
crystal system	triclinic
a [Å]	11.045(4)
b [Å]	15.670(6)
c [Å]	17.674(6)
α [°]	75.901(8)
β [°]	85.286(8)
γ [°]	88.395(8)
V [Å^3]	2956.7(18)
T [K]	293(2)
space group	$P\bar{1}$
Z	2
μ($Mo_{K\alpha}$) [mm^{-1}]	6.249
θ range [°]	1.19–23.26°
reflections collected	14291
unique reflections/R_{int}	8490/0.0661]
$R1$[a]/$wR2$[b] ($I>2\sigma$)	0.0656/0.1470
$R1$[a]/$wR2$[b] (all data)	0.1173/0.1714
max. shift/esd	0.006
residual ρ [e A^{-3}]	2.399/−1.834

[a] $R1=\Sigma||F_o|-|F_c||/\Sigma F_o$. [b] $wR2=[\Sigma[w(F_o^2-F_c^2)^2]/\Sigma[w(F_o^2)^2]]^{1/2}$.

software was used for absorption correction.[34,35] Final cell parameters were obtained by global refinement of 907 reflections for **3**-$BPh_4\cdot CH_2Cl_2$ obtained from integration of all the frames data. The crystal parameters and basic information relating to data collection and structure refinement are summarized in Table 3.

The structures were solved by direct methods and refined by the full-matrix method based on F^2 using the SHELXTL software package.[36] The non-hydrogen atoms were refined anisotropically; the positions of all hydrogen atoms were generated geometrically, assigned isotropic thermal parameters and allowed to ride on their respective parent carbon atoms. The final difference Fourier map in the structure of **3**-$BPh_4\cdot CH_2Cl_2$ showed the presence of one molecule of CH_2Cl_2 which was refined as a rigid group.

CCDC-215667 contains the supplementary crystallographic data for this paper. These data can be obtained free of charge via www.ccdc.cam.ac.uk/conts/retrieving.html (or from the Cambridge Crystallographic Data Centre, 12 Union Road, Cambridge CB2 1EZ, UK; fax: (+44) 1223-336-033; or deposit@ccdc.cam.ac.uk).

Acknowledgement

Financial support by the Spanish Dirección General de Enseñanza Superior (Research Projects BQ2000-232 and BQU2002-00313), Junta de Andalucía (Grupo FQM-137), and Generalitat Valenciana (Research Project CTIDIB/2002/330) is gratefully acknowledged. We also thank Prof. R. Poli (Universite de Bourgogne) and Prof. M. Martínez (Universitat de Barcelona) for helpful suggestions during the preparation of the manuscript.

[1] a) R. Hernández-Molina, A. G. Sykes, *J. Chem. Soc. Dalton Trans.* **1999**, 3137; b) R. Llusar, S. Uriel, *Eur. J. Inorg. Chem.* **2003**, 1271–1290.
[2] E. I. Stiefel, K. Matsumoto, *Transition Metal Sulfur Chemistry*, ACS Symposium Series, Honolulu (Hawaii), **1995**.
[3] Q.-F. Zhang, Y.-N. Xiong, T.-S. Lai, W. Ji, X.-Q. Xin, *J. Phys. Chem. B* **2000**, *104*, 3446.
[4] M. Feliz, J. M. Garriga, R. Llusar, S. Uriel, M. G. Humphrey, N. T. Lucas, M. Samoc, B. Luther-Davies, *Inorg. Chem.* **2001**, *40*, 6132.
[5] M. Nasreldin, A. Olatunji, P. W. Dimmock, A. G. Sykes, *J. Chem. Soc. Dalton Trans.* **1990**, 1765.
[6] D. M. Saysell, V. P. Fedin, G. J. Lamprecht, M. Sokolov, A. G. Sykes, *Inorg. Chem.* **1997**, *36*, 2982.
[7] F. A. Cotton, R. Llusar, C. T. Eagle, *J. Am. Chem. Soc.* **1989**, *111*, 4332.
[8] E. A. Quadrelli, H. B. Kraatz, R. Poli, *Inorg. Chem.* **1996**, *35*, 5154, and references therein.
[9] J. F. Coetzee, *Prog. Phys. Org. Chem.* **1967**, *4*, 45.
[10] M. G. Basallote, J. Durán, M. J. Fernández-Trujillo, M. A. Máñez, J. Rodríguez de la Torre, *J. Chem. Soc. Dalton Trans.* **1998**, 745.
[11] E. J. Moore, J. M. Sullivan, J. R. Norton, *J. Am. Chem. Soc.* **1986**, *108*, 2257.
[12] a) G. Parkin, J. E. Bercaw, *J. Chem. Soc. Chem. Commun.* **1989**, 255; b) K. E. Oglieve, R. A. Henderson, *J. Chem. Soc. Chem. Commun.* **1992**, 441; c) R. A. Henderson, K. E. Oglieve, *J. Chem. Soc. Dalton Trans.* **1993**, 3431.
[13] R. G. Wilkins, *Kinetics and Mechanisms of Reactions of Transition Metal Complexes*, VCH, New York, **1991**, Chapter 1, p. 22.
[14] a) W. Marty, J. H. Espenson, *Inorg. Chem.* **1979**, *18*, 1246 ; b) M. C. Pohl, J. H. Espenson, *Inorg. Chem.* **1980**, *19*, 235 ;c) J. P. Bourke, E. Kart, R. D. Canon, *Inorg. Chem.* **1996**, *35*, 1577 ; d) M. G. Basallote, J. Durán, M. J. Fernández-Trujillo; M. A. Máñez, *J. Chem. Soc. Dalton Trans.* **1999**, 3817.
[15] a) F. A. Armstrong, R. A. Henderson, A. G. Sykes, *J. Am. Chem. Soc.* **1980**, *102*, 6545; b) P. Kathirgamanathan, A. B. Soares, D. T. Richens, A. G. Sykes, *Inorg. Chem.* **1985**, *24*, 2950; c) B. L. Ooi, A. G. Sykes, *Inorg. Chem.* **1988**, *27*, 310.
[16] F. A. Cotton, P. A. Kibala, M. Matusz, C. S. McCaleb, R. B. W. Sandor, *Inorg. Chem.* **1989**, *28*, 2623.
[17] K. Hegetschweiler, M. Wörh, M. D. Meienberger, R. Nesper, H. W. Schmalle, R. D. Hancock, *Inorg. Chim. Acta* **1996**, *250*, 35.
[18] M. Sasaki, G. Sakane, T. Ouchi, T. Shibahara, *J. Cluster Sci.* **1998**, *9*, 25.
[19] L. M. Epstein, E. S. Shubina, *Coord. Chem. Rev.* **2002**, *231*, 165, and references therein.
[20] a) A. A. González, K. Zhang, C. D. Hoff, *Inorg. Chem.* **1989**, *28*, 4295; b) J. M. Millar, R. V. Kastrup, M. T. Melchior, I. V. Horvath, C. D. Hoff, R. H. Crabtree, *J. Am. Chem. Soc.* **1990**, *112*, 9643; c) K. Zhang, A. A. González, S. L. Mukerjee, S. Chou, K. A. Kubat-Martin, D. Barnhart, G. J. Kubas, *J. Am. Chem. Soc.* **1991**, *113*, 9170.
[21] M. G. Basallote, J. Durán, M. J. Fernández-Trujillo, M. A. Máñez, *J. Chem. Soc. Dalton Trans.* **1998**, 3227.
[22] See for example: a) G. R. Dukes, R. H. Holm, *J. Am. Chem. Soc.* **1975**, *97*, 528; b) J. L. C. Duff, J. L. J. Breton, J. N. Butt, F. A. Armstrong, A. J. Thomson, *J. Am. Chem. Soc.* **1996**, *118*, 8593; c) R. A. Henderson, K. E. Oglieve, *J. Chem. Soc. Dalton Trans.* **1998**, 1731.
[23] M. G. Basallote, J. Durán, M. J. Fernández-Trujillo, M. A. Máñez, *J. Chem. Soc. Dalton Trans.* **1998**, 2205.
[24] M. G. Basallote, J. Durán, M. J. Fernández-Trujillo, M. A. Máñez, *Inorg. Chem.* **1999**, *38*, 5067.
[25] M. G. Basallote, J. Durán, M. J. Fernández-Trujillo, M. A. Máñez, *J. Organomet. Chem.* **2000**, *609*, 29.
[26] a) R. P. Bell, *The Proton in Chemistry*, Cornell University Press, Ithaca, NY, 1973, p. 200; b) K. J. Laidler, *Chemical Kinetics, 3rd ed.*, Harper & Row, New York, **1987**.
[27] M. G. Basallote, J. Durán, M. J. Fernández-Trujillo, M. A. Máñez, *Organometallics* **2000**, *19*, 695.
[28] F. Estevan, M. Feliz, R. Llusar, J. A. Mata, S. Uriel, *Polyhedron* **2001**, *20*, 527.
[29] GLINT Software, *Applied Photophysics Ltd.*, Leatherhead, **1995**.
[30] A. D. Becke, *J. Chem. Phys.* **1993**, *98*, 5648.
[31] C. Lee, Y. Yang, R. G. Parr, *Phys. Rev. Sect. B* **1988**, *37*, 785.
[32] M. J. Frisch, G. W. Trucks, H. B. Schlegel, G. E. Scuseria, M. A. Robb, J. R. Cheeseman, V. G. Zakrzewski, J. A. Montgomery Jr., R. E. Stratmann, J. C. Burant, S. Dapprich, J. M. Millam, A. D. Daniels, K. N. Kudin, M. C. Strain, O. Farkas, J. Tomasi, V. Barone, M. Cossi, R. Cammi, B. Mennucci, C. Pomelli, C. Adamo, S. Clifford, J. Ochterski, G. A. Petersson, P. Y. Ayala, Q. Cui, K. Morokuma, D. K. Malick, A. D. Rabuck, K. Raghavachari, J. B. Foresman, J. Cioslowski, J. V. Ortiz, A. G. Baboul, B. B. Stefanov, G. Liu, A. Liashenko, P. Piskorz, I. Komaromi, R. Gomperts, R. L. Martin, D. J. Fox, T. Keith, M. A. Al-Laham, C. Y. Peng, A. Nanayakkara, C. Gonzalez, M. Challacombe, P. M. W. Gill, B. Johnson, W. Chen, M. W. Wong,

J. L. Andres, C. Gonzalez, M. Head-Gordon, E. S. Replogle, J. A. Pople, in 'Gaussian 98', Pittsburgh, PA, **1998**.
[33] P. J. Hay, R. Wadt, *J. Chem. Phys.* **1985**, *82*, 270.
[34] SAINT, 5.0 ed.; Bruker Analytical X-ray Systems: Madison, WI, **1996**.
[35] G. M. Sheldrick, SADABS empirical absorption program, University of Göttingen, 1996.
[36] G. M. Sheldrick, SHELXTL, 5.1 ed., Brucker Analytical X-Ray Systems, Madison, WI., **1997**.

Received: July 24, 2003
Revised: October 2, 2003 [F5376]

